www.nature.com/ismej

ISME

ARTICLE

Check for updates

Light-driven carbon dioxide reduction to methane by *Methanosarcina barkeri* in an electric syntrophic coculture

Lingyan Huang[1,3], Xing Liu[1,3], Zhishuai Zhang[1], Jie Ye[1], Christopher Rensing[1✉], Shungui Zhou[1✉] and Kenneth H. Nealson[2]

The direct conversion of CO_2 to value-added chemical commodities, thereby storing solar energy, offers a promising option for alleviating both the current energy crisis and global warming. Semiconductor-biological hybrid systems are novel approaches. However, the inherent defects of photocorrosion, photodegradation, and the toxicity of the semiconductor limit the application of these biohybrid systems. We report here that *Rhodopseudomonas palustris* was able to directly act as a living photosensitizer to drive CO_2 to CH_4 conversion by *Methanosarcina barkeri* under illumination after coculturing. Specifically, *R. palustris* formed a direct electric syntrophic coculture with *M. barkeri*. Here, *R. palustris* harvested solar energy, performed anoxygenic photosynthesis using sodium thiosulfate as an electron donor, and transferred electrons extracellularly to *M. barkeri* to drive methane generation. The methanogenesis of *M. barkeri* in coculture was a light-dependent process with a production rate of 4.73 ± 0.23 μM/h under light, which is slightly higher than that of typical semiconductor-biohybrid systems (approximately 4.36 μM/h). Mechanistic and transcriptomic analyses showed that electrons were transferred either directly or indirectly (via electron shuttles), subsequently driving CH_4 production. Our study suggests that *R. palustris* acts as a natural photosensitizer that, in coculture with *M. barkeri*, results in a new way to harvest solar energy that could potentially replace semiconductors in biohybrid systems.

The ISME Journal (2022) 16:370–377; https://doi.org/10.1038/s41396-021-01078-7

INTRODUCTION

The past few decades have witnessed a continuous increase in CO_2 emissions due to the use of nonrenewable hydrocarbon fuels [1]. The ever-increasing anthropogenic energy demand has further aggravated the CO_2 content in the atmosphere [2], exacerbating global warming and climate change [3, 4]. This issue has led to a number of approaches for the direct capture and conversion of CO_2, including physical, chemical, and biological methods [5–7]. Among them, the direct conversion of CO_2 to value-added compounds, such as energy fuels, shows great promise. In these approaches, catalysts, such as rare metals and enzymes, are usually required to facilitate the conversion of CO_2 [8–10]. However, low product selectivity, poor sustainability, and intensive energy investment have often limited their applications [11, 12]. Another option is to use whole-microbe biocatalysts, taking advantage of the highly organized pathways that favor the multistep CO_2 fixation process and operate under the protection of the cell envelope [8, 13].

Energy investment is necessary to drive CO_2 fixation in whole-cell biocatalytic systems [14]. Green energy, such as solar light, is thought to be the best choice [15]. Initial attempts have involved the construction of photoelectrochemical semiconductor biohybrids [16–18]. In these systems, semiconductor electrodes are used to harvest light and produce photoexcited electrons that are then "fed" to autotrophic bacteria via the cathode and serve as reducing power for CO_2 fixation. However, strong illumination is required to excite the semiconductor electrode for electron generation, and the inefficient electron transfer between the electrode and microbes often limits the operational efficiency of the system [15]. In contrast, photosynthetic semiconductor biohybrids display efficient electron transfer and contribute to high solar-to-chemical efficiency [13, 19–21]. In biohybrids, light-harvesting semiconducting nanomaterials integrate whole-cell biocatalysts by forming intimate connections on/in microbial cells [20, 22, 23]. Thereafter, photoelectrons directly enter the reductive pathway and drive reducing power generation. Such biohybrids represent the best available mimics of photosynthesis in photosynthetic bacteria and provide potential solutions for nonphotosynthetic autotrophic bacteria to combine solar energy harvesting and CO_2 fixation. Unfortunately, the innate defects of semiconductors, including cytotoxicity, photocorrosion, photodegradation, and the generation of photoexcited radicals, and their irreproducibility impair the stability and sustainability of biohybrids [15, 24, 25].

Photosynthetic bacteria house both light-harvesting elements and CO_2-fixation machinery. Several photosynthetic bacteria, such as cyanobacteria and microalgae, have been selected as platforms to perform photosynthesis for CO_2 to value-added product conversion [7, 26, 27]. Even though the natural photoreaction center in a photosynthetic bacterium is much more efficient in light absorption and energy conversion than any of the

[1]Fujian Provincial Key Laboratory of Soil Environmental Health and Regulation, College of Resources and Environment, Fujian Agriculture and Forestry University, Fuzhou, China. [2]Department of Earth Science, University of Southern California, Los Angeles, CA, USA. [3]These contributed equally: Lingyan Huang, Xing Liu ✉email: rensing@iue.ac.cn ; sgzhou@fafu.edu.cn

Received: 8 February 2021 Revised: 21 July 2021 Accepted: 22 July 2021
Published online: 2 August 2021

man-made photosensitizers, with an ability to be excited by a wide light spectrum and intensity, the carbon fixation pathway in photosynthetic bacteria is often less energetically favorable than that in lithoautotrophs [28, 29]. One potential solution to this problem involves the combination of the light-harvesting center of photosynthetic bacteria with the CO_2-fixation machinery of nonphotosynthetic bacteria via the construction of a hybrid system to achieve efficient solar light-driven CO_2 fixation. Notably, pioneering attempts have been performed by expressing the photoreaction center and allowing photophosphorylation in a nonphotosynthetic heterotrophic bacterium [30].

Rhodopseudomonas palustris is a purple nonsulfur photosynthetic bacterium that has been reported to generate current or reduce iron (III) oxides under illumination [31, 32], suggesting an ability to generate photoelectrons and transfer these electrons extracellularly. We speculated that *R. palustris* might be able to be used as a "natural whole-cell photosensitizer." Here, we report the verification of this speculation by coculturing *R. palustris* with *Methanosarcina barkeri* to drive the conversion of CO_2 to CH_4. *M. barkeri* was chosen for study because: (1) it has been previously reported to directly accept electrons from other bacterial species, such as the exoelectrogen *Geobacter metallireducens* [33], after forming a direct electron syntrophic coculture to reduce CO_2 for CH_4 generation, and (2) because CH_4 is a potential renewable energy source. In the coculture, both time-dependent and light-dependent methanogenesis were evaluated, and it was concluded that *R. palustris* and *M. barkeri* formed electron syntrophic cocultures to perform CO_2-to-CH_4 conversion. That is, *R. palustris* acted as a photosensitizer harvesting solar energy and producing electrons to drive the formation of methane in *M. barkeri*, and suggesting that such a photosynthetic coculture may provide an alternate strategy to replace semiconductors with photosynthetic bacteria in biohybrids.

MATERIALS AND METHODS

Bacterial strains and cultivation condition

R. palustris strain CGMCC 1.2180 was purchased from the China General Microbiological Culture Collection Center. *M. barkeri* MS (DSM 800) was purchased from the German Collection of Microorganisms and Cell Cultures. Strains of *R. palustris* and *M. barkeri* were routinely cultured in 0259 medium and CSM medium [34], respectively, at 35 °C under anaerobic conditions (N_2:CO_2, 80:20). In particular, *R. palustris* was cultured under illumination by LED light (15 W, with a wavelength of 590–592 nm and optical power density of 20 W m^{-2} measured by an optical power meter (CEL-NP2000, CEAULIGHT, Beijing)). When *R. palustris* and *M. barkeri* grew to their late exponential stages, cells were collected and washed three times using 0.9% NaCl solution by centrifuging at 6500 ×g for 15 min at 4 °C. The washed cells were used to initiate coculture by inoculating *R. palustris* and *M. barkeri* cells into 30 mL USM medium [34] without cysteine but supplied with 2 mM thiosulfate, achieving a final OD_{600} of 0.1, with thiosulfate as the only electron donor and CO_2 as the sole electron acceptor. CH_4 and H_2 production by coculture were monitored as previously described using a gas chromatograph (Agilent 7890A, USA) with an HP-5 column and flame ionization detector [34]. The lowest detection limit for H_2 is 50 ppm.

Operation of photosynthetic microbial fuel cells (photo-MFCs)

Two-chamber H-cells were employed to construct photosynthetic microbial fuel cells (photo-MFCs) as previously reported [35]. Briefly, the cell had a liquid volume of 25 mL and a headspace volume of 5 mL for each chamber. Graphite plates with a size of 1.5 cm × 1 cm × 0.5 cm were used as the electrodes. A proton exchange membrane (Nafion 117, DuPont Co., USA) was used to separate the anodic and cathodic chambers. An external resistance (1 MΩ) was applied between the anode and cathode, and the voltage across the resistance was recorded every 2 min by a data acquisition system (model 2700, Keithley Instruments, Ohio, USA), which was used to calculate the current density. USM medium (without cysteine) supplied with 2 mM thiosulfate served as the electrolyte. To initiate the reactions, 1 mL of *R. palustris* and *M. barkeri* cells (OD_{600} = 0.3) were inoculated into the anodic and cathodic chambers separately. The photo-MFCs were incubated at 30 °C under illumination by LED light, except the cathodic chamber containing *M. barkeri* was wrapped with aluminum foil to maintain darkness. The biofilms formed on anodic and cathodic electrodes were stained using a BacLight Live/Dead kit following the manufacturer's instructions (Life Technologies, USA).

Electrochemical measurements

Linear sweep voltammetry (LSV) analysis of *R. palustris* and *M. barkeri* was performed using a single-chamber three-electrode cell as previously described [36]. A 4 cm × 5 cm indium tin-oxide glass was placed at the bottom and served as the working electrode. A platinum wire and Hg|Hg_2Cl_2 (sat. KCl) electrode were used as the counter and reference electrodes, respectively, and the electrolyte was USM medium (without cysteine) except supplying 2 mM thiosulfate for the *R. palustris* culture. LSV was conducted using an electrochemical workstation (660E, CH instruments, USA) and scanning over the range from −1 to 0.6 V at a rate of 1 mV s^{-1}. Differential pulse voltammetry (DPV) analysis of the culture supernatant was conducted in the same setup. The parameters were E_i = −0.8 V, E_f = 0.3 V, pulse height 50 mV, pulse width 250 ms, step height 2 mV, step time 500 ms, and scan rate 5 mV s^{-1}.

Physically separated culture cell setup

The physically separated culture cell was a modification of the photo-MFC setup with a semipermeable membrane (molecular weight cutoff of 1 kDa) replacing the proton exchange membrane and without electrodes (Supplementary Fig. S1). To start the operation of the cell, 0.5 mL of *R. palustris* and *M. barkeri* cells (OD_{600} = 0.3) were separately injected into the anodic and cathodic chambers. Both chambers were stirred continuously with stir bars.

Microscopy and fluorescent in situ hybridization

An optical microscope (Nikon Eclipse E200, Japan) operating in phase-contrast mode was employed to observe the cocultured cells grown at their logarithmic phase under a 100× objective lens. Fluorescent in situ hybridization was performed as previously described [37]. The probe 5′-[CY3]GCTGCCTCCCGTAGGAGT-3′ was selected for *R. palustris*, and the probe 5′-[CY5]GTGCTCCCCCGCCAATTCCT-3′ was used to label *M. barkeri*. Images were obtained using a confocal laser scanning microscope with a 40× objective lens (LSM880 NLO, ZEISS).

Quantification of *R. palustris*

The amount of *R. palustris* was absolutely quantified by quantitative PCR. Briefly, genomic DNA was extracted using TIANamp Bacteria DNA kit (Tiangen, Beijing, China). *R. palustris*-specific gene was amplified using the primer pair RpFor (5′-CTGGAAGTCTTGAGTATGGC-3′) and RpRev (5′-GCCTCAGCGTCAGTAATGGC-3′), and was cloned into the pMD19-T vector for a standard curve calculation. Quantitative PCR using the same primer pair was performed as previously described via a LightCycler 480 System (Roche Applied Science, Penzberg, Germany) [37].

Transcriptomic analysis

Cocultured cells at the early mid-log phase were collected by centrifugation at 5000 ×g for 15 min at 4 °C. Total RNA was extracted using TRIzol reagent (Invitrogen, California, USA) as previously described [38]. Directional libraries were prepared with the NEBNext® Ultra II™ Directional RNA Library Prep Kit (New England Biolabs Ltd., Beijing, China). mRNA was then sequenced by performing paired-end sequencing with the Illumina HiSeq/MiSeq paltformsOpen. All raw sequencing data were quality checked and filtered as previously described [39]. All reads matching 16S and 23S rRNA genes were removed, and the remaining reads were then used to map against the published genome of *R. palustris* CGMCC 1.2180 (NZ_CP058907.1) and *M. barkeri* MS (NZ_CP009528.1). Mapped reads were normalized with fragments per kilobase per million mapped reads (FPKM) as previously reported [39, 40].

RESULTS

Light-driven methanogenesis in *R. palustris* and *M. barkeri* coculture

R. palustris and *M. barkeri* were cocultured in a defined coculture medium with thiosulfate as the sole electron donor, carbon dioxide as the only electron acceptor and light as the energy

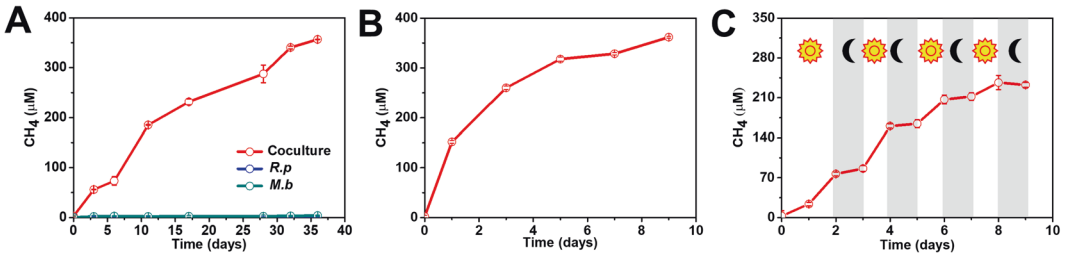

Fig. 1 Methanogenesis in *R. palustris* (*R.p*) and *M. barkeri* (*M.b*) cocultures. Methane accumulation after initial inoculation (**A**) and at the sixth transfer after being transferred five times (**B**). **C** Methane production by *R. palustris* and *M. barkeri* coculture during continuous light-dark cycling.

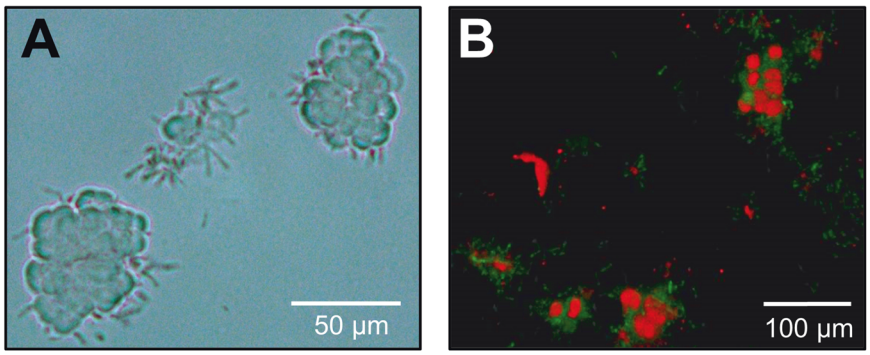

Fig. 2 *R. palustris* and *M. barkeri* coculture aggregates. A Phase-contrast microscopy image and **B** fluorescence in situ hybridization (FISH) image. *R. palustris* was detected by a green probe, and *M. barkeri* was labeled by a red probe.

source. As illustrated in Fig. 1A, neither *R. palustris* nor *M. barkeri* could produce methane alone in the coculture medium. In contrast, their coculture generated methane steadily, approaching 357 ± 14 μM after 36 days (Fig. 1A). After continuous transfer, the methane generation rate increased, achieving 362 ± 11 μM after 9 days (Fig. 1B) in the sixth transfer with a calculated rate of 4.73 ± 0.23 μM/h, suggesting the formation of a stable methanogenic coculture. Furthermore, methane generation in the coculture was light-dependent, being activated by light and inhibited in darkness (Fig. 1C). *R. palustris* is in the purple nonsulfur group of bacteria that perform cyclic photophosphorylation and are incapable of methane formation [41]. Thus, *R. palustris* could not produce methane in the coculture medium. Instead, it performed as an anaerobic anoxygenic photoautotroph by oxidizing thiosulfate for CO_2 fixation in the coculture medium (Supplementary Fig. S2A) [42]. In particular, under illumination, *R. palustris* could oxidize thiosulfate and transfer electrons extracellularly when an electron acceptor, such as an anode, was present (Supplementary Fig. S2B), as had been previously reported [32]. Furthermore, in the coculture, the presence of the extracellular electron acceptor in the form of *M. barkeri* promoted the photoautotrophy of *R. palustris* (Supplementary Fig. S3), probably by balancing the intracellular redox status, suggesting a syntrophic relationship between those two species.

M. barkeri can use H_2, acetate, and some one-carbon compounds to produce methane [43]. However, H_2 should not be produced by *R. palustris* in the system, as H_2 was shown to be the byproduct of biological nitrogen fixation in *R. palustris*, which would be inhibited in the presence of abundant ammonium in the culture medium [44]. As expected, no H_2 was detected in the system (data not shown). Furthermore, neither acetate nor one-carbon compounds were generated by *R. palustris* as evidence by the fact that no methanogenesis was seen when *M. barkeri* was incubated in the filtrate of *R. palustris* monoculture spent medium (data not shown). Given that *M. barkeri* has been reported to take up electrons from electron-donating *Geobacter* species to reduce CO_2 for methane production [33, 45], we propose that *R. palustris* acted as an electron donor in the light to drive the methanogenesis of *M. barkeri* in the coculture.

To establish the origin of the methane, ^{13}C isotope labeling analysis was performed by replacing the ^{12}C-$NaHCO_3$ in the coculture medium with ^{13}C-labeled $NaHCO_3$, and the headspace gas was collected for gas chromatography–mass spectrometry analysis. As expected, ^{13}C appeared in CH_4, suggesting the direct CO_2 to CH_4 conversion in the coculture (Supplementary Fig. S4).

LSV analysis of *R. palustris* and *M. barkeri* demonstrated that *R. palustris* could transfer electrons outwards in a potential range of greater than −0.62 V (vs. SHE), while *M. barkeri* could accept electrons inwards in a potential range of less than 0.57 V. Thus, theoretically, electrons could transfer from *R. palustris* to *M. barkeri* in a potential window from −0.62 to 0.57 V (vs. SHE) (Fig. 3A) when applicable electrical conduits existed. These results suggest the possibility of electromethanogenesis of *M. barkeri* driven by electrons produced by *R. palustris* in the coculture. Actually, the two species formed aggregates (Fig. 2), a characteristic of electrosyntrophic coculture, in which microbial species are directly connected with each other providing an electron connection for direct interspecies electron transfer [37, 38].

Interspecies electron transfer between *R. palustris* and *M. barkeri*

To identify the process of electromethanogenesis in the coculture, *R. palustris* and *M. barkeri* were separately inoculated into each chamber of a MFC and then electrically connected by an external circuit as previously reported [35]. Both species formed biofilms on the electrodes (Supplementary Fig. S5), indicating direct electron transfer between either species and the electrode, as previously reported [35], and produced a maximum current of approximately 0.6 mA/m^2 (Fig. 3B) with an accumulated CH_4 production of 50.25 ± 3.32 μM after 30 days (Fig. 3C). As expected, this current production showed positive light activation (Fig. 3D). Notably, under darkness, a lower current was still produced (Fig. 3D), which was attributed to the consumption of stored energy by *R. palustris* since *R. palustris* could not oxidize thiosulfate by performing

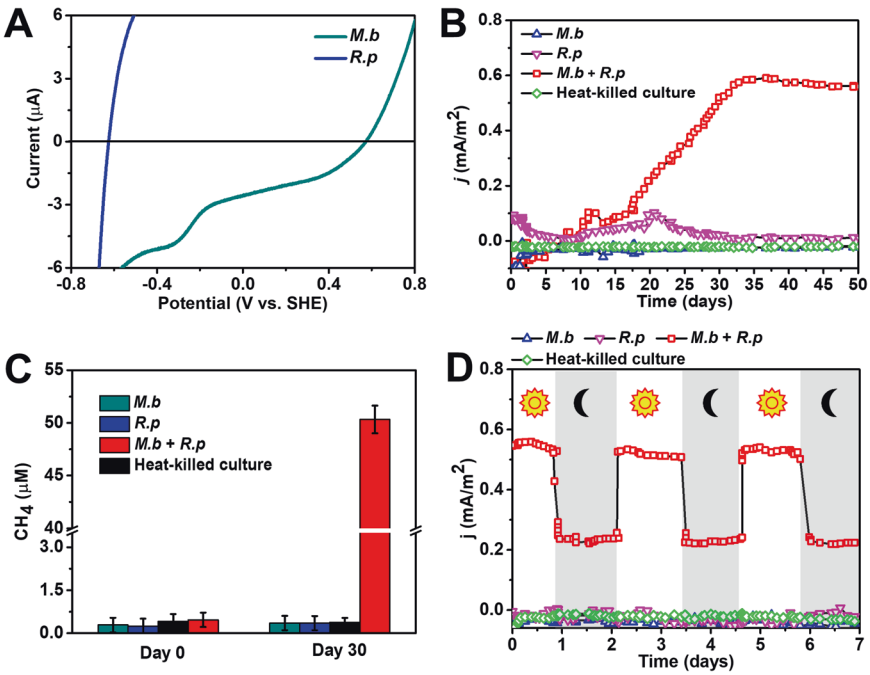

Fig. 3 Direct electrosyntrophic methanogenesis between *R. palustris* and *M. barkeri*. **A** Linear sweep voltammetry analysis. *R. palustris* generated anodic current in a potential range of greater than −0.62 V, and *M. barkeri* produced a cathodic current in a potential range of less than 0.57 V. **B** Current generation of photo-MFCs with an external resistance of 1 MΩ, showing direct electron transfer from the *R. palustris* anode to the *M. barkeri* cathode. The current generation of monocultures of *R. palustris* in the anode chamber and *M. barkeri* in the cathode chamber and of the two species in the separated chambers were measured. **C** Corresponding methane production in the photo-MFCs, showing that electrons produced by *R. palustris* could directly drive methanogenesis of *M. barkeri*. **D** Current generation of photo-MFCs during alternate light-dark cycles, showing light-driven electron transfer between *R. palustris* and *M. barkeri*. The test was performed after a steady current was generated.

anaerobic chemotrophy under darkness (data not shown). In contrast, neither monocultures nor heat-killed cocultures produced current and methane (Fig. 3B, C) or displayed a current response to light (Fig. 3D). These results demonstrate that *R. palustris* acted as a photosensitizer, harvesting light energy and releasing electrons that *M. barkeri* could use for methane generation and suggesting direct interspecies electron transfer between those two species in coculture, since the proton exchange membrane excluded possible electron exchange for methanogenesis between the two species.

Microbial cells have been reported to secrete electron carriers or electron mediators to facilitate interspecies electron transfer [46, 47]. The possibility of meditated interspecies electron transfer between the two species was tested in a two-chamber cell separated by a semipermeable membrane that only allowed molecules with a molecular weight lower than 1 kDa to pass (Supplementary Fig. S1). Under these circumstances, these two species could not directly connect to transfer electrons. As indicated in Fig. 4A, 47.05 ± 7.36 μM of CH_4 was produced by separated *R. palustris* and *M. barkeri* cultures in 35 days. In contrast, neither single species nor dead cells produced methane (Fig. 4A). The results demonstrate the possibility of indirect interspecies electron transfer facilitated by electron mediators between *R. palustris* and *M. barkeri* to support methanogenesis.

DPV analysis of cell-free culture medium was performed further to identify potential redox electron mediators. As shown in Fig. 4B, two redox compounds were detected with peak potentials at −0.28 and 0.01 V (vs. SHE) in the physically separated cultures, both of which lie in the potential window (−0.62 to 0.57 V vs. SHE), which would allow the electron transfer from *R. palustris* to *M. barkeri*. In contrast, no redox peaks were identified in the culture medium from monocultures of either *R. palustris* or *M. barkeri* or from the heat-killed separated cultures. However, the redox compound of 0.01 V should not contribute to the methanogenesis of *M. barkeri* since the potential is too high to drive the reduction of CO_2 to methane (E^0 of $CO_2/CH_4 = -0.24$ V) [48]. These results indicate that when separated, the methanogenic culture could produce redox compounds to mediate interspecies electron transfer. Coincidentally, two humic-like compounds (corresponding to fluorescence peaks I and II with excitation/emission of 270/435 and 340/430, respectively) were also identified by three-dimensional excitation–emission matrix fluorescence spectroscopy (Fig. 4C), but they were absent in the fluorescence spectrum of the plain culture medium and the culture media having grown with either species (Supplementary Fig. S6). Humic-like compounds have been reported to be redox active and can be secreted by microbial cells, facilitating extracellular electron transfer (EET) and mediating interspecies electron transfer [49, 50]. Therefore, redox-active compounds, such as humic-like substances, mediated interspecies electron transfer between physically separated *R. palustris* and *M. barkeri*. The same tests were also performed on the culture medium from aggregated coculture. Only a small redox peak with a potential at 0.01 V was detected in the differential pulse voltammogram (Supplementary Fig. S7), and a faint emission peak that was assigned to the 340/430 excitation/emission pair appeared (Supplementary Fig. S6), indicating that humic-like compounds were not highly secreted and did not significantly promote methanogenesis of the coculture. Therefore, direct interspecies electron transfer dominated in the aggregated coculture.

Electrosyntrophic CO_2 reduction to CH_4 by *M. barkeri* in coculture

Transcriptomic analyses were performed to dissect the light-driven electrosyntrophic methanogenesis in the coculture. The $\log_2$ FPKM value of each gene transcript was calculated and

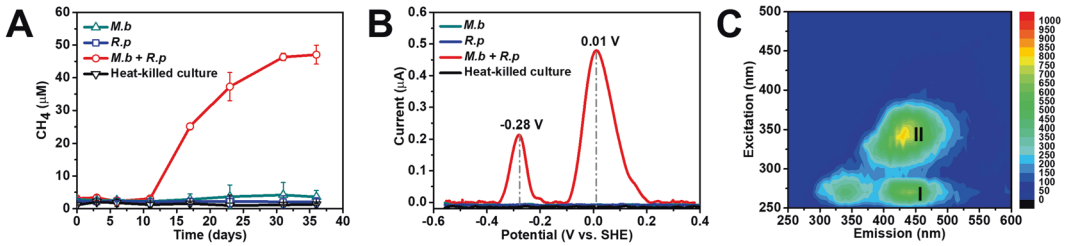

Fig. 4 Indirect interspecies electron transfer between *R. palustris* and *M. barkeri*. **A** Methane production by physically separated *R. palustris* and/or *M. barkeri* cultures, indicating the possibility of indirect electron transfer between these two species. **B** Baseline subtracted differential pulse voltammogram of the cell-free culture supernatant from physically separated culture cells, showing the presence of at least two redox-active compounds that could act as electron shuttles to facilitate electron transfer between *R. palustris* and *M. barkeri*. **C** Three-dimensional fluorescence spectrum of the culture supernatants from physically separated *R. palustris* and *M. barkeri* cultures. The two fluorescence peaks (I and II) correspond to the fluorescence of humic-like compounds.

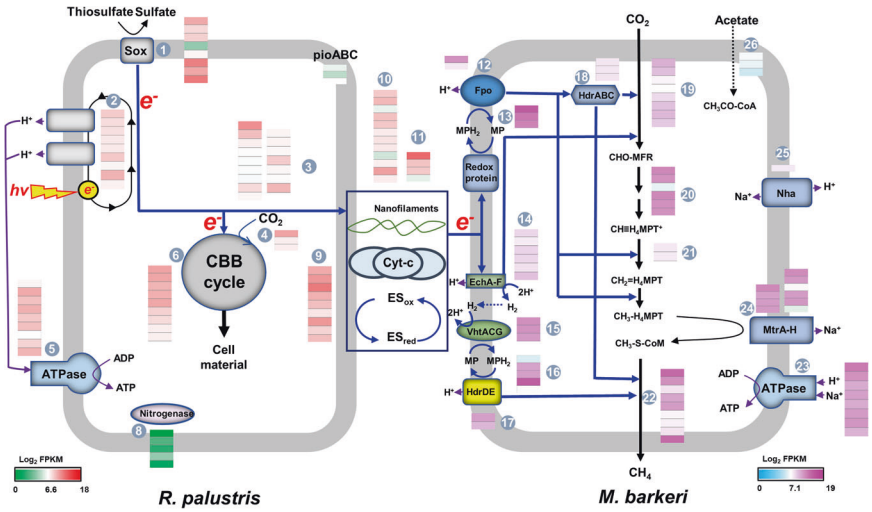

Fig. 5 The mechanism of light-driven CO_2-to-CH_4 conversion in *R. palustris* and *M. barkeri* coculture as revealed by metatranscriptomics. Genes involved in the processes include those that encode (1) Sox proteins, (2) proteins involved in cyclic photophosphorylation, (3) NADH-quinone oxidoreductase, (4) Ribulose-1,5-bisphosphate carboxylase/oxygenase, (5) and (23) ATP synthase, (6) enzymes participating in the Calvin–Benson–Bassham cycle, (7) PioABC, (8) nitrogenases, (9) c-type cytochromes, (10) flagellar proteins, (11) pilus proteins, (12) $F_{420}H_2$ dehydrogenases Fpo, (13) and (16) proteins involved in methanophenazine biosynthesis, (14) EchA-F hydrogenases, (15) MP-reducing hydrogenases VhtACG, (17) heterodisulfide reductases HdrDE, (18) heterodisulfide reductases HdrABC, (19) Formylmethanofuran dehydrogenases, (20) F420 hydrogenases, (21) Methenyl cyclohydrolases, (22) Methyl-CoM reductases, (24) methyltransferases MtrA-H, (25) Na^+/H^+ antiporter Nha, (26) acyl-CoA synthetases. Inset heat maps show the average transcript abundance of genes from triplicate independent cocultures presented as $\log_2$ FPKM values. The median $\log_2$ FPKM was 6.6 for *R. palustris* and 7.1 for *M. barkeri*. The blue and red lines indicate the speculated electron flux and CO_2 fixation pathway, respectively, during light-driven methanogenesis in the coculture.

compared with the median (6.6 and 7.1 for *R. palustris* and *M. barkeri*, respectively) to evaluate gene expression (Supplementary Table S1). In *R. palustris*, sulfite oxidase (Sox) is responsible for thiosulfate oxidation, and ribulose-1,5-bisphosphate carboxylase/oxygenase (RubisCO) and enzymes involved in the Calvin–Benson–Bassham cycle are responsible for autotrophic CO_2 fixation. The cyclic photophosphorylation pathway for energy generation was highly expressed (Fig. 5), consistent with *R. palustris* performing anoxygenic photoautotrophic growth by oxidizing thiosulfate under light in coculture. Previous reports have demonstrated that the membrane protein complex of PioAB and periplasmic protein PioC serve as part of the EET conduit to accept electrons from Fe(II) minerals and cathode in *R. palustris* [51, 52]. Surprisingly, the gene cluster *pioABC* was not highly expressed, suggesting that the pathways utilized for electron output by *R. palustris* were different from the one utilized for electron uptake. In contrast, flagella, pili, and some outer membrane c-type cytochromes were highly expressed (Fig. 5). The nanofilaments of flagella or pili in *R. palustris* have been reported to be conductive [31], and both conductive nanofilaments and cytochromes could participate in direct interspecies electron transfer [33, 37]. Therefore, the results are consistent with and suggestive of the direct electron interaction between *R. palustris* and *M. barkeri* and suggest that nanofilaments and cytochromes are involved in interspecies electron transfer in the coculture.

Two membrane-bound hydrogenases, ferredoxin-dependent hydrogenase (Ech) and methanophenazine-dependent hydrogenase (Vht), and the membrane-bound heterodisulfide reductase complex (HdrDE) were highly expressed in *M. barkeri* (Fig. 5). Ech and Vht represent the energy-converting mechanism of *M. barkeri* by running intracellular H_2 cycling to drive the reduction of methanophenazine (MP) [45, 53]. Thereafter, the redox cycling of MP/MPH_2 provides electrons to the membrane-bound heterodisulfide reductase complex (HdrDE) for the reduction of CoM-S-S-CoB [45, 54]. In particular, the membrane-bound Ech complex was proposed to provide the interface to receive photoelectrons released by the semiconductor to drive CO_2-to-CH_4 conversion in the methanogenesis biohybrid system [34]. Therefore, membrane hydrogenase-dependent intracellular H_2 cycling could provide an electron transfer mechanism for methanogenesis of *M. barkeri* in the coculture. In addition, both the proton-pumping

F_{420}-dehydrogenase (Fpo) and methanophenazine biosynthesis genes were highly expressed. In the absence of hydrogenase, the Fpo-dependent electron transfer pathway has been reported to support the growth of *M. barkeri*, providing a hydrogenase-independent electron transport pathway of direct electron uptake from extracellular electron sources [55, 56]. Under these circumstances, membrane-bound methanophenazine could contribute not only to the electrical conductivity of the membrane but also to MP/MPH_2 cycling and thereafter mediate electron transfer from membrane-bound redox active protein to the Fpo-complex [57, 58]. Therefore, MP-Fpo could also serve as the electron uptake channel for *M. barkeri* in the coculture. Furthermore, Fpo could catalyze the generation of $F_{420}H_2$, which would participate in the electron bifurcation reaction catalyzed by the cytoplasmic heterodisulfide reductase complex (HdrABC) and contribute to the generation of reduced ferredoxin and the reduction of CoM-S-S-CoB, as indicated by the high expression of HdrABC. Consistent with these results, the CO_2-to-CH_4 conversion pathway was highly expressed, while the acetate degradation pathway was not (Fig. 5), which was also in agreement with electrosyntrophic CO_2 reduction to CH_4 by *M. barkeri*, as previously reported [39].

DISCUSSIONS

Here we have provided the first proof that *R. palustris* can be used as a whole-cell photosensitizer to harvest light energy to drive the methanogenesis of *M. barkeri*. Under illumination, *R. palustris* and *M. barkeri* aggregated and formed an electrosyntrophic coculture in which *R. palustris* harvested light energy and performed photoautotrophy by oxidizing thiosulfate and transferring electrons extracellularly. Subsequently, *M. barkeri* accepted these electrons and used them for the reduction of CO_2 to CH_4. Furthermore, the electrons could be transferred between the two species either directly by cytochromes and conductive filaments or indirectly via electron shuttles in the form of humic-like substances. Such versatility of interspecies electron transfer may suggest that there will be a broad spectrum of electrosyntrophic partners for *R. palustris*.

The coculture system combines the strengths of both microbial species, which includes the highly efficient light-harvesting center in *R. palustris* and the highly specific methanogenic apparatus in *M. barkeri*, not only showing a higher thermodynamic favorability than hydrogen-dependent methanogenesis [59] but also having advantages over other light-driven methanogenic systems. For example, an abiotic artificial photosynthetic cell was designed employing the cathode catalyst and a platinum decorated semiconductive anode that harvested light energy for water splitting and provided electrons for CO_2 to CH_4 reduction on the cathode [60]. However, this system is not environmental and energy benign since precious metal and an external electric potential had to be applied in the system. In addition, even though the cathode catalyst has a relative high selectivity, without regarding its stability and persistence after long-time operation, its synthetic process is complex and harsh needing a high temperature of 800 °C. Similarly, in inorganic-biological hybrid systems, conventional semiconductor photosensitizers, such as the widely used CdS, demonstrate inherent defects in terms of photocorrosion, photodegradation, and toxicity, limiting their sustainability. In contrast, in the coculture system, the living photosensitizer of *R. palustris* confers sustainability, biocompatibility, self-replication, and self-repair. Moreover, the coculture produced methane at a highest rate of 4.73 ± 0.23 μM/h, which is higher than all reported biohybrid methanogenesis systems (3.46 μM/h for CdS@*M. barkeri* and approximately 3.81–4.36 μM/h for CdS:Ni@*M. barkeri*) [34, 61] and even higher than the engineered *R. palustris* methanogenic mutant (approximately 3 μM/h) [62], indicating effectiveness and efficiency. Notably, sacrificial organic reagents, such as alcohol and cysteine, are necessary to act as ultimate electron donors in biohybrid systems. In contrast, the inorganic substance thiosulfate donated electrons in our methanogenic coculture, which provided electrons for CO_2 fixation to generate organic matter in *R. palustris* and for CO_2 reduction to CH_4 in *M. barkeri*, suggesting zero CO_2 emissions in the *R. palustris* and *M. barkeri* electrosyntrophic coculture. Furthermore, previous attempts have employed *R. palustris* as a photosensitizer to harvest solar energy for current generation [32]. However, in our study, solar energy was stored as chemical energy in biomass and methane, representing a more efficient energy storage strategy.

Our study suggested the proof-of-concept of using living photosensitizers of anoxygenic photosynthetic bacteria to drive nonphotosynthetic microbial CO_2 fixation. While thiosulfate was used as the electron donor in our methanogenic coculture, it is possible to use other electron donors, such as the universal electron donors H_2 and Fe^{2+} minerals [63], or other low-value organics such as acetate or glycerol [32] to perform EET under light. Meanwhile, some nonphotosynthetic autotrophic bacteria, such as acetogens like *Clostridium ljungdahlii* or *Moorella thermoacetica* [64], have been shown to use extracellular electrons for CO_2 reduction. Actually, those autotrophic bacteria being the workhorse of synthetic biology have shown great promise to act as platforms for CO_2 being used in the production of tailored value-added compounds in microbial electrosynthesis and have been used in constructing biohybrids [15]. Thus, it can be predicted that *R. palustris* should be capable of serving as a living photosensitizer to drive CO_2 conversion to value-added products, not limited to CH_4, in those autotrophic bacteria via the formation of the electrosyntrophic coculture. Specially, photosynthetic organisms, such as algae and plant, have been shown to achieve direct light-harvesting and CO_2 reduction to conversion to value-added compounds [65]. However, model prediction indicated that algal and cellulosic bioenergy programs aggravate global warming caused by nitrous oxide arising from the extensive use of fertilizers [65, 66]. Furthermore, thermodynamic comparison indicated that the carbon fixation pathway in those photosynthetic organisms is often less energetically favorable [29], which is in contrast to versatile autotrophic carbon fixation pathways with cheaper energy-consumption in nonphotosynthetic autotrophic bacteria. Notably, in the coculture system, solar energy and extracellular electrons were just partially flowed into those value-added products since they also supported the photoautotrophic growth of *R. palustris* in the electrosyntrophic coculture. Modulating the electron flow toward EET in *R. palustris* should increase the productivity of the coculture system.

The formation of an electrosyntrophic interaction benefits both species in the coculture. *R. palustris* is a metabolically versatile microbe that uses a wide electron donor spectrum ranging from inorganic substances to complex organic matter. In contrast, *M. barkeri* is only able to use several one- to two-carbon compounds or hydrogen. Considering that the presence of the electron acceptor strain *M. barkeri* promoted the anoxygenic photosynthesis of *R. palustris*, the electrosyntrophic interaction could improve the resilience of both species in nature. Actually, in some natural methanogenesis hotspots, such as paddy soil [67], wetland [68], and coastal zones [69], anaerobic photosynthetic bacteria prevail. It can be speculated that the solar light-driven methanogenesis between anaerobic photosynthetic bacteria and methanogens should also prevail in these environments, contributing to global carbon cycling. Repeatedly, the emergence of EET has been shown to open up a wide variety of new metabolic "windows" that simply were not imagined until a few years ago. In particular, EET between different microbial species has expanded the range of electron donor or acceptor being possible from one species to another species, contributing the formation of highly cooperated microbial communities with specific functions. Recently, electrosyntrophy has been discovered in various microbial communities, from bacteria [37] to archaea [70] and

even in some conventional hydrogen syntrophic communities [71]. Our study has further extended the family of electrosyntrophic species and we are confident will inspire the discovery of electrosyntrophy in other microbial communities.

REFERENCES

1. Dong K, Hochman G, Govinda RT. Do drivers of CO_2 emission growth alter overtime and by the stage of economic development? Energy Policy. 2020;140:11420.
2. Butti SK, Mohan SV. Autotrophic biorefinery: dawn of the gaseous carbon feedstock. FEMS Microbiol Lett. 2017;364.
3. Ryouta OI, Ayako AO. Influence of dynamic vegetation on climate change arising from increasing CO_2. Clim Dyn. 2009;33:645–63.
4. Ghommem M, Hajj MR, Puri IK. Influence of natural and anthropogenic carbon dioxide sequestration on global warming. Ecol Model. 2012;235-236:1–7.
5. Bhatia SK, Bhatia RK, Jeon J-M, Kumar G, Yang Y-H. Carbon dioxide capture and bioenergy production using biological system—a review. Renew Sustain Energy Rev. 2019;110:143–58.
6. Cheah WY, Ling TC, Juan JC, Lee DJ, Chang JS, Show PL. Biorefineries of carbon dioxide: from carbon capture and storage (CCS) to bioenergies production. Bioresour Technol. 2016;215:346–56.
7. Salehizadeh H, Yan N, Farnood R. Recent advances in microbial CO_2 fixation and conversion to value-added products. Chem Eng J. 2020;390:124584–603.
8. White JL, Baruch MF, Pander Iii JE, Hu Y, Fortmeyer IC, Park JE, et al. Light-driven heterogeneous reduction of carbon dioxide: photocatalysts and photoelectrodes. Chem Rev. 2015;23:12888–935.
9. Chang X, Wang T, Gong J. CO_2 photo-reduction: insights into CO_2 activation and reaction on surfaces of photocatalysts. Energy Environ Sci. 2016;9:2177–96.
10. Kong Q, Kim D, Liu C, Yu Y, Su Y, Li Y, et al. Directed assembly of nanoparticle catalysts on nanowire photoelectrodes for photoelectrochemical CO_2 reduction. Nano Lett. 2016;16:5675–80.
11. Ross MB, De Luna P, Li Y, Dinh C-T, Kim D, Yang P, et al. Designing materials for electrochemical carbon dioxide recycling. Nat Catal. 2019;2:648–58.
12. Varela AS, Ju W, Reier T, Strasser P. Tuning the catalytic activity and selectivity of Cu for CO_2 electroreduction in the presence of halides. ACS Catal. 2016;6:2136–44.
13. Fang X, Kalathil S, Reisner E. Semi-biological approaches to solar-to-chemical conversion. Chem Soc Rev. 2020;49:4926–52.
14. Otsuki T. A study for the biological CO_2 fixation and utilization system. Sci Total Environ. 2001;277:21–25.
15. Cestellos-Blanco S, Zhang H, Kim JM, Shen Y-X, Yang P. Photosynthetic semiconductor biohybrids for solar-driven biocatalysis. Nat Catal. 2020;3:245–55.
16. Nichols EM, Gallagher JJ, Liu C, Su Y, Chang CJ. Hybrid bioinorganic approach to solar-to-chemical conversion. Proc Natl Acad Sci USA. 2015;112:11461–6.
17. Fu Q, Xiao S, Li Z, Li Y, Kobayashi H, Li J, et al. Hybrid solar-to-methane conversion system with a Faradaic efficiency of up to 96%. Nano Energy. 2018;53:232–9.
18. Liu C, Gallagher JJ, Sakimoto KK, Nichols EM, Chang CJ, Chang MCY, et al. Nanowire–bacteria hybrids for unassisted solar carbon dioxide fixation to value-added chemicals. Nano Lett. 2015;15:3634–9.
19. Kornienko N, Sakimoto KK, Herlihy DM, Nguyen SC, Alivisatos AP, Harris CB, et al. Spectroscopic elucidation of energy transfer in hybrid inorganic–biological organisms for solar-to-chemical production. Proc Natl Acad Sci USA. 2016;113:11750–5.
20. Sakimoto KK, Wong AB, Yang P. Self-photosensitization of nonphotosynthetic bacteria for solar-to-chemical production. Science. 2016;351:74–7.
21. Kornienko N, Zhang JZ, Sakimoto KK, Yang P, Reisner E. Interfacing nature's catalytic machinery with synthetic materials for semi-artificial photosynthesis. Nat Nanotechnol. 2018;13:890–9.
22. Guo J, Suástegui M, Sakimoto KK, Moody VM, Xiao G, Nocera DG, et al. Light-driven fine chemical production in yeast biohybrids. Science. 2018;362:813–6.
23. Zhang H, Liu H, Tian Z, Lu D, Yu Y, Cestellos-Blanco S, et al. Bacteria photosensitized by intracellular gold nanoclusters for solar fuel production. Nat Nanotechnol. 2018;13:900–5.
24. Hossain ST, Mukherjee SK. Toxicity of cadmium sulfide (CdS) nanoparticles against *Escherichia coli* and HeLa cells. J Hazard Mater. 2013;260:1073–82.
25. Wang C, Wang L, Jin J, Liu J, Li Y, Wu M, et al. Probing effective photocorrosion inhibition and highly improved photocatalytic hydrogen production on monodisperse PANI@CdS core-shell nanospheres. Appl Catal B-Environ. 2016;188:351–9.
26. Parmar A, Singh NK, Pandey A, Gnansounou E, Madamwar D. Cyanobacteria and microalgae: a positive prospect for biofuels. Bioresour Technol. 2011;102:10163–72.
27. Knoot CJ, Ungerer J, Wangikar PP, Pakrasi HB. Cyanobacteria: promising biocatalysts for sustainable chemical production. J Biol Chem. 2018;293:5044–52.
28. Boyle NR, Morgan JA. Computation of metabolic fluxes and efficiencies for biological carbon dioxide fixation. Metab Eng. 2011;13:150–8.
29. Fast AG, Papoutsakis ET. Stoichiometric and energetic analyses of non-photosynthetic CO_2-fixation pathways to support synthetic biology strategies for production of fuels and chemicals. Curr Opin Chem Eng. 2012;1:380–95.
30. Martinez A, Bradley AS, Waldbauer JR, Summons RE, DeLong EF. Proteorhodopsin photosystem gene expression enables photophosphorylation in a heterologous host. Proc Natl Acad Sci USA. 2007;104:5590–5.
31. Venkidusamy K, Megharaj M, Schröder U, Karouta F, Mohan SV, Naidu R. Electron transport through electrically conductive nanofilaments in *Rhodopseudomonas palustris* strain RP2. RAC Adv. 2015;5:100790–8.
32. Xing D, Zuo Y, Cheng S, Regan JM, Logan BE. Electricity generation by *Rhodopseudomonas palustris* DX-1. Environ Sci Technol. 2008;42:4146–51.
33. Rotaru AE, Shrestha PM, Liu F, Markovaite B, Chen S, Nevin KP, et al. Direct interspecies electron transfer between *Geobacter metallireducens* and *Methanosarcina barkeri*. Appl Environ Microbiol. 2014;80:4599–605.
34. Ye J, Yu J, Zhang Y, Chen M, Liu X, Zhou S, et al. Light-driven carbon dioxide reduction to methane by *Methanosarcina barkeri*-CdS biohybrid. Appl Catal B-Environ. 2019;257:117916.
35. Huang L, Liu X, Tang J, Yu L, Zhou S. Electrochemical evidence for direct interspecies electron transfer between *Geobacter sulfurreducens* and *Prosthecochloris aestuarii*. Bioelectrochemistry. 2019;127:21–5.
36. Kato S, Hashimoto K, Watanabe K. Microbial interspecies electron transfer via electric currents through conductive minerals. Proc Natl Acad Sci USA. 2012;109:10042–6.
37. Liu X, Zhuo S, Rensing C, Zhou S. Syntrophic growth with direct interspecies electron transfer between pili-free *Geobacter* species. ISME J. 2018;12:2142–51.
38. Shrestha PM, Rotaru AE, Aklujkar M, Liu F, Shrestha M, Summers ZM, et al. Syntrophic growth with direct interspecies electron transfer as the primary mechanism for energy exchange. Environ Microbiol Rep. 2013;5:904–10.
39. Rotaru AE, Shrestha PM, Liu F, Shrestha M, Shrestha D, Embree M, et al. A new model for electron flow during anaerobic digestion: direct interspecies electron transfer to *Methanosaeta* for the reduction of carbon dioxide to methane. Energy Environ Sci. 2013;7:408–15.
40. Holmes DE, Shrestha PM, Walker DJF, Dang Y, Nevin KP, Woodard TL, et al. Metatranscriptomic evidence for direct interspecies electron transfer between *Geobacter* and *Methanothrix* species in methanogenic rice paddy soils. Appl Environ Microbiol. 2017;83:00223–17.
41. Mckinlay JB, Harwood CS. Carbon dioxide fixation as a central redox cofactor recycling mechanism in bacteria. Proc Natl Acad Sci USA. 2010;107:11669–75.
42. Zheng Y, Harris DF, Yu Z, Fu Y, Poudel S, Ledbetter RN, et al. A pathway for biological methane production using bacterial iron-only nitrogenase. Nat Microbiol. 2018;3:281–6.
43. Wu W, Meador TB, Könneke M, Elvert M, Wegener G, Hinrichs KU. Substrate-dependent incorporation of carbon and hydrogen for lipid biosynthesis by *Methanosarcina barkeri*. Environ Microbiol Rep. 2020;12:555–67.
44. Fixen KR, Chowdhury NP, Martinez-Perez M, Poudel S, Boyd ES, Harwood CS. The path of electron transfer to nitrogenase in a phototrophic alphaproteobacterium. Environ Microbiol. 2018;20:2500–8.
45. Holmes DE, Rotaru AE, Ueki T, Shrestha PM, Ferry JG, Lovley DR. Electron and proton flux for carbon dioxide reduction in *Methanosarcina barkeri* during direct interspecies electron transfer. Front Microbiol. 2018;9:3109.
46. Shrestha PM, Rotaru AE. Plugging in or going wireless: strategies for interspecies electron transfer. Front Microbiol. 2014;5:237.
47. Huang L, Liu X, Ye Y, Chen M, Zhou S. Evidence for the coexistence of direct and riboflavin-mediated interspecies electron transfer in *Geobacter* co-culture. Environ Microbiol. 2020;22:243–54.
48. Drake HL, Küsel K, Matthies C. Acetogenic prokaryotes. In: Dworkin M, Falkow S, Rosenberg E, Schleifer K-H, Stackebrandt E, editors. The prokaryotes: volume 2: ecophysiology and biochemistry. New York, NY: Springer New York; 2006. p. 354–420.
49. Wang S, Wu Y, An J, Liang D, Li N. *Geobacter* autogenically secretes fulvic acid to facilitate the dissimilated iron reduction and vivianite recovery. Environ Sci Technol. 2020;17:10850–8.
50. Smith JA, Nevin KP, Lovley DR. Syntrophic growth via quinone-mediated interspecies electron transfer. Front Microbiol. 2015;6:121.
51. Bose A, Gardel EJ, Vidoudez C, Parra EA, Girguis PR. Electron uptake by iron-oxidizing phototrophic bacteria. Nat Commun. 2014;5:3391.
52. Guzman MS, Rengasamy K, Binkley MM, Jones C, Ranaivoarisoa TO, Singh R, et al. Phototrophic extracellular electron uptake is linked to carbon dioxide fixation in the bacterium *Rhodopseudomonas palustris*. Nat Commun. 2019;10:1355.

53. Mand T, Kulkarni G, Metcalf W. Genetic, biochemical, and molecular characterization of *Methanosarcina barkeri* mutants lacking three distinct classes of hydrogenase. J Bacteriol. 2018;20:e00342–00318.
54. Li Q, Li L, Rejtar T, Lessner DJ, Karger BL, Ferry JG. Electron transport in the pathway of acetate conversion to methane in the marine archaeon *Methanosarcina acetivorans*. J Bacteriol. 2006;188:702–10.
55. Welte C, Deppenmeier U. Bioenergetics and anaerobic respiratory chains of aceticlastic methanogens. Biochim Biophys Acta. 2014;1837:1130–47.
56. Kulkarni G, Mand TD, Metcalf WW. Energy conservation via hydrogen cycling in the methanogenic archaeon *Methanosarcina barkeri*. mBio. 2018;9:e01256–18.
57. Duszenko N, Buan NR. Physiological evidence for isopotential tunneling in the electron transport chain of methane-producing archaea. Appl Environ Microbiol. 2017;83:e00950–00917.
58. Yan Z, Joshi P, Gorski CA, Ferry JG. A biochemical framework for anaerobic oxidation of methane driven by Fe(III)-dependent respiration. Nat Commun. 2018;9:1642.
59. Storck T, Virdis B, Batstone DJ. Modelling extracellular limitations for mediated versus direct interspecies electron transfer. ISME J. 2016;10:621–31.
60. Xuan X, Cheng J, Yang X, Zhou J. Highly selective electrochemical reduction of CO_2 to CH_4 over vacancy–metal–nitrogen sites in an artificial photosynthetic cell. ACS Sustain Chem Eng. 2020;8:1679–86.
61. Ye J, Ren G, Kang L, Zhang Y, Liu X, Zhou S, et al. Efficient photoelectron capture by Ni decoration in *Methanosarcina barkeri*-CdS biohybrids for enhanced photocatalytic CO_2-to-CH_4 conversion. iScience. 2020;23:101287.
62. Ma L, Fang Z, Wang Y-Z, Zhou J, Yong Y-C. Photo-driven highly efficient one-step CO_2 biomethanation with engineered photo-synthetic bacteria *Rhodopseudomonas palustris*. *ACS Sustain*. Chem Eng. 2020;8:9616–21.
63. Jiao Y, Newman DK. The pio operon is essential for phototrophic Fe(II) oxidation in *Rhodopseudomonas palustris* TIE-1. J Bacteriol. 2007;189:1765–73.
64. Nevin KP, Hensley SA, Franks AE, Summers ZM, Ou J, Woodard TL, et al. Electrosynthesis of organic compounds from carbon dioxide is catalyzed by a diversity of acetogenic microorganisms. Appl Environ Microbiol. 2011;77:2882–6.
65. Clarens AF, Resurreccion EP, White MA, Colosi LM. Environmental life cycle comparison of algae to other bioenergy feedstocks. Environ Sci Technol. 2010;44:1813–9.
66. Melillo JM, Reilly JM, Kicklighter DW, Gurgel AC, Cronin TW, Paltsev S, et al. Indirect emissions from biofuels: how important? Science. 2009;326:1397–9.
67. Harada N, Nishiyama M, Matsumoto S. Inhibition of methanogens increases photo-dependent nitrogenase activities in anoxic paddy soil amended with rice straw. FEMS Microbiol Ecol. 2001;35:231–8.
68. He S, Malfatti SA, McFarland JW, Anderson FE, Pati A, Huntemann M, et al. Patterns in wetland microbial community composition and functional gene repertoire associated with methane emissions. mBio. 2015;6:e00066–15.
69. Broman E, Sun X, Stranne C, Salgado MG, Bonaglia S, Geibel M, et al. Low abundance of methanotrophs in sediments of shallow boreal coastal zones with high water methane concentrations. Front Microbiol. 2020;11:1536.
70. McGlynn SE, Chadwick GL, Kempes CP, Orphan VJ. Single cell activity reveals direct electron transfer in methanotrophic consortia. Nature. 2015;526:531–5.
71. Walker DJF, Nevin KP, Holmes DE, Rotaru A-E, Ward JE, Woodard TL, et al. Syntrophus conductive pili demonstrate that common hydrogen-donating syntrophs can have a direct electron transfer option. ISME J. 2020;14:837–46.

ACKNOWLEDGEMENTS

This work was supported by the National Science Fund for Distinguished Young Scholars of China, grants no. 41925028, the National Natural Science Foundation of China, grant no. 42077218, the Project of Fujian Provincial Department of Science and Technology of China, grant no. 2020J01568, and the Fujian Agriculture and Forestry University Program for Distinguished Young Scholar, grant no. xjq202001.

AUTHOR CONTRIBUTIONS

LH and XL conceived and designed the study; LH and ZZ performed the experiments and collected the data; XL drew all figures and wrote the manuscript; XL, CR, SZ, and KHN analyzed and interpreted the data; JY and KHN revised the manuscript. All authors reviewed, revised, and approved the final manuscript.

COMPETING INTERESTS

The authors declare no competing interests.

ADDITIONAL INFORMATION

Supplementary information The online version contains supplementary material available at https://doi.org/10.1038/s41396-021-01078-7.

Correspondence and requests for materials should be addressed to C.R. or S.Z.

Reprints and permission information is available at http://www.nature.com/reprints

Publisher's note Springer Nature remains neutral with regard to jurisdictional claims in published maps and institutional affiliations.